THE JOURNAL OF PHYSICAL CHEMISTRY B

 VOLUME 112, NUMBER 28, JULY 17, 2008

ARTICLES

Antioxidant Nanoreactor Based on Superoxide Dismutase Encapsulated in Superoxide-Permeable Vesicles

Fabian Axthelm,[†] Olivier Casse,[†] Willem H. Koppenol,[‡] Thomas Nauser,[‡] Wolfgang Meier,[†] and Cornelia G. Palivan*,[†]

Department of Chemistry, University of Basel, Klingelbergstrasse 80, CH-4056 Basel, Switzerland, and Institute of Inorganic Chemistry, Department of Chemistry and Applied Bioscience, ETH, CH-8093 Zurich, Switzerland

Received: April 8, 2008; Revised Manuscript Received: April 21, 2008

We designed and tested an antioxidant nanoreactor based on encapsulation of Cu,Zn superoxide dismutase in amphiphilic copolymer nanovesicles, the membranes of which are oxygen permeable. The nanovesicles, made of poly(2-methyloxazoline)−poly(dimethylsiloxane)−poly(2-methyloxazoline), successfully encapsulated the protein during their self-assembling process, as proved by confocal laser-scanning microscopy and fluorescence-correlation spectroscopy. Electron paramagnetic resonance spectroscopy and circular dichroism analyses showed that no structural changes appeared in the protein molecules once inside the inner space of the nanovesicles. The function of this antioxidant nanoreactor was tested by pulse radiolysis, which demonstrated that superoxide dismutase remains active inside the nanovesicles and detoxifies the superoxide radical in situ. The membrane of our triblock copolymer nanovesicles plays a double role, both to shield the sensitive protein and to selectively let superoxide and dioxygen penetrate to its inner space. This simple and robust hybrid system provides a selective shielding of sensitive enzymes from proteolytic attack and therefore a new direction for developing drug delivery applications.

Introduction

Efficient strategies for the regulation of partially reduced oxygen species (PROS), including cellular antioxidants, such as glutathione and ascorbate, and enzymes, such as glutathione peroxidase, glutathione transferases, catalase, and superoxide dismutase (SOD), exist in living cells. In certain pathologies, the production of PROS overwhelms cellular antioxidant defense mechanisms leading to oxidative stress. PROS, which include the superoxide radical anion ($O_2^{\bullet -}$), peroxynitrite, the hydroxyl radical, and hydrogen peroxide, are constantly produced in living organisms and are involved in the initiation and progression of chronic inflammation. Oxidative stress has been shown to play a significant role in many disease states including arthritis, Parkinson's disease, amyotrophic lateral sclerosis, cancer, and AIDS.[1–4]

Cu,Zn-SOD is known to decrease the steady-state concentration of superoxide radicals and could be a suitable candidate drug; it is, however, quickly eliminated from the bloodstream (6 min in rats and 30 min in humans)[5] and poorly adsorbed from and rapidly degraded in the gastrointestinal tract,[4] thereby compromising its delivery. Attempts have been made to improve delivery by protecting the protein (i) with the hydroxyl radical

* E-mail: Cornelia.Palivan@unibas.ch.
[†] University of Basel.
[‡] ETH Zurich.

10.1021/jp803032w CCC: $40.75
Published on Web 06/21/2008

scavengers homocarnosine or anserine,[6] (ii) by covalent modification with polyethylene glycol (PEG)[7] or sodium chondroitin sulfate,[8] and (iii) by encapsulation into liposomes.[9–11] Although modification with PEG represents one of the most conventional ways to protect an enzyme from proteolytic attack, excessive covalent modification can compromise activity.[12] Likewise, encapsulation of SOD into liposomes has serious drawbacks, such as significant leakage due to structural defects,[13] mechanical instability, interaction with high-density lipoproteins,[14] and a short circulation lifetime.[15]

Another way, which emerged these last years, for protection of sensitive proteins consists in shielding the protein in polymeric carriers that contain an internal space; the system of cage and encapsulated protein has been named a nanoreactor if the protein is acting in situ.[16,17] Various types of polymerosome nanoreactors have been developed, either by changing the nature and the combination of block copolymers or to address different applications based on an enzyme or combination of enzymes.[18–20] Unlike liposome-based carriers, the polymeric vesicles have morphologies and properties that may be controlled by the high diversity of block copolymers. This approach allows the variation of the chemical constitution, length of different blocks, or molecular architecture of the whole copolymer, which makes them more versatile for a wider range of applications.[21] A simple and robust approach to prepare polymeric drug carriers is to use amphiphilic copolymers which self-assembly in aqueous solutions into vesicular structures. In a fashion analogous to that for lipids.[22]They consist of spherical closed block-copolymer membranes with diameters in the range from 50 nm to approximately 10 μm, depending on the chemical constitution, size of polymer blocks, preparation method, and reaction conditions.[23] The polymer vesicles thus obtained are significantly more stable against lysis by classical surfactants than liposomes because of the low entropy of mixing of polymers while preserving the low immunogenicity.[24,25] In addition, the vast amount of available blocks makes it possible to tune their properties, such as wall thickness, polarity, toxicity, or sensor-responsivity.[16,26] To the best of our knowledge, as yet, no nanoreactors that function as antioxidants have been proposed. There have been attempts to encapsulate SOD in polymeric carriers, but in the conventional approach of drug delivery, the enzyme acts only after its release from the carrier.[27,28]

We propose here a new strategy to detoxify the $O_2^{\bullet-}$ based on encapsulation of Cu,Zn-SOD in oxygen-permeable nanovesicles formed by self-assembly of amphiphilic triblock copolymer. Herein, we describe the design and analysis of antioxidant nanoreactors prepared from poly(2-methyloxazoline)−poly(dimethylsiloxane)−poly(2-methyloxazoline), PMOX−PDMS−PMOXA,[29] that encapsulates Cu,Zn-SOD as shown in Figure 1. The chosen block copolymers have a proven record of good biocompatibility,[30] and the hydrophilic PMOXA block shows low nonspecific protein binding ability.[31] The polymer membrane of these nanovesicles is stable and impermeable to saccharide ions and water[32] and demonstrates none of the sort of organizational defects responsible for the known instability of liposomal drug carriers.[13] Our nanoreactor is not limited to use with SOD; any compound or combination of compounds having antioxidant properties may be encapsulated.

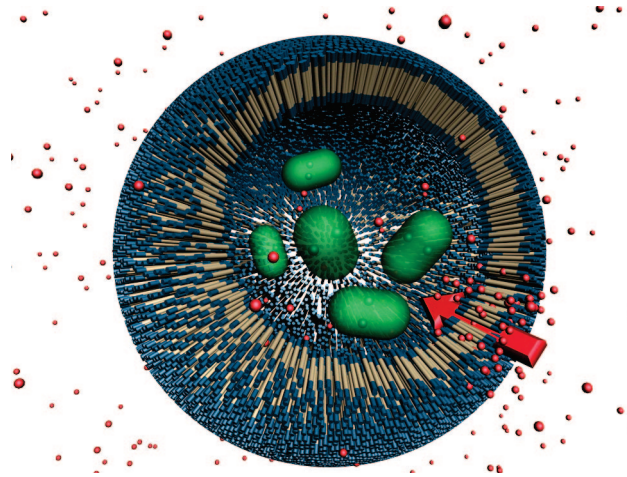

Figure 1. Schematic representation of an antioxidant nanoreactor with encapsulated SOD. The $O_2^{\bullet-}$ is able to penetrate the polymeric shield.

Materials and Methods

Materials. Cu,Zn-SOD from bovine erythrocytes (Sigma Aldrich), Alexa Fluor 488 (Invitrogen), dimethylsulfoxide (DMSO; Aldrich), Sephadex G-50 (Fluka), and ethanol (99.8%; Fluka) were used without any further treatment. Sepharose 4B (Sigma Aldrich) and polycarbonate membrane filters (Millipore, 200 nm) were used. Alexa Fluor 488 (Invitrogen) was used as described in the manufacturer's protocol (MP00143, http://www.invitrogen.com).

Nanovesicle Preparation. The synthesis of $PMOXA_n-PDMS_m-PMOXA_n$ (where $n = 15$ and $m = 110$), has been described elsewhere.[32] Nanovesicles were prepared according to a modification of a previously published method.[33] The triblock copolymer $PMOXA_{15}-PDMS_{110}-PMOXA_{15}$ (50 mg) was dissolved in ethanol at 17% (w/w) and stirred at room temperature for 1 h. After complete dissolution, this solution was slowly added dropwise to phosphate-buffered saline (PBS) buffer to give a final polymer concentration of 10 mg/mL, and the mixture was stirred overnight at room temperature. The solution was then extruded 20 times through a polycarbonate membrane filter (Millipore) with a well-defined pore size of 200 nm to decrease the size polydispersity of vesicles.[33] Subsequently, the extruded solution was purified by size-exclusion chromatography (SEC) on Sepharose 4B (10 × 300 mm).

Fluorescence Labeling of SOD. Fluorescently labeled SOD was obtained by reaction of Alexa Fluor 488 with the primary amines of the protein. Labeled SOD was separated from unbound Alexa Fluor 488 by SEC on Sephadex G50 (10 × 300 mm) equilibrated with PBS buffer. The concentration of labeled protein in solution was determined by pulse radiolysis.[34] The number of Alexa Fluor 488/SOD molecule was determined by fluorescence corelation spectroscopy.

Encapsulation of Fluorescently Labeled SOD in Nanovesicles. Encapsulated SOD was obtained by adding the polymer solution as described above to a solution of labeled SOD (0.26 mg/mL) in PBS buffer. The nonencapsulated protein was removed by size exclusion chromatography on a Sepharose 4B column, with the same buffer. To determine whether the protein can be attacked from outside the vesicles, a stock solution of 20 mg/mL of proteinase K (Roche) was added to the solution of encapsulated, fluorescently labeled SOD at 5% (v:v), and the mixture was incubated for 4 h at room temperature.

Light Scattering. Dynamic (DLS) and static (SLS) light-scattering experiments to determine the sizes and size distribution of empty and SOD-containing polymeric nanovesicles were performed on a ALV (Langen, Germany) goniometer, equipped with an ALV He−Ne laser ($\lambda = 632.8$ nm). SOD-encapsulated

and empty nanovesicles were prepared by serial dilution to polymer concentrations ranging from 3.33 to 0.1 mg/mL. Light scattering was measured in 10 mm cylindrical quartz cells at angles of 30−150° at 293 K. The data for DLS were analyzed by using a Williams−Watts function.[35] The size polydispersity of the vesicles was determined according to the literature.[36–38]

Transmission Electron Microscopy (TEM). Nanovesicle dispersions (empty vesicles and vesicles containing encapsulated SOD-Alexa Fluor 488) were negatively stained with 2% uranyl acetate solution and deposited on a carbon-coated copper grid. The samples were examined with a transmission electron microscope (Philips Morgagni 268D) at 293 K.

Laser-Scanning Microscopy/Fluorescence-Correlation Spectroscopy. Laser-scanning microscopy (LSM) and fluorescence-correlation spectroscopy (FCS) measurements were obtained with a Zeiss LSM 510-META/Confcor2 laser-scanning microscope equipped with an argon laser (488 nm) and a 40× water-immersion objective (Zeiss C/Apochromat 40X, NA 1.2), with the pinhole adjusted to 70 μm. Solutions of polymeric nanoreactors (2−3 mg/mL) with encapsulated SOD-Alexa Fluor 488 were measured at room temperature in special chambered quartz-glass holders (Laboratory-Tek; 8-well, NUNC A/S) that provide optimal conditions for imaging while reducing evaporation of the aqueous solutions. In LSM mode, appropriate filters were chosen, and the detector gain, amplifier gain, and offset were adjusted to optimize micrograph quality; images (512 × 512 pixels) were collected with a scan speed of 0.96 s/pixel at 8-bit color depth. In FCS mode, intensity fluctuations were analyzed in terms of an autocorrelation function with the LSM 510/Confocor software package (Zeiss, AG). Spectra were recorded over 30 s, and each measurement was repeated 10 times; results are reported as the average of three independent experiments. Adsorption and bleaching effects were reduced by exchanging the sample droplet after 5 min of measurement. The excitation power of the Ar laser was $P_L = 15$ mW, and the excitation transmission at 488 nm was 2%. To reduce the number of free fitting parameters, the diffusion times for free dye (Alexa Fluor 488) as well as the labeled SOD were independently determined and fixed in the fitting procedure.

Circular Dichroism. Circular dichroism (CD) spectra (180−260 nm) were recorded to determine the impact of the labeling and encapsulation conditions on the SOD molecule. Measurements were made with an Applied Photophysics Chirascan CD spectrometer. Encapsulated SOD-Alexa Fluor 488 collected from the SEC purification step was treated with a centrifugal filter device (Centricon YM-10, Millipore, 10 kDa nominal molecular weight cutoff) at 5000 g to exchange the PBS buffer with MilliQ water (18 MΩ cm; Purelab UHQ, Elga) and compared with unlabeled SOD solubilized in MilliQ water.

Electron Paramagnetic Resonance Spectroscopy. Electron paramagnetic resonance (EPR) spectra were recorded at 77 K with a CW Bruker ElexSys500 X-band CW spectrometer, equipped with a helium temperature control system (ER4112HV), to which the resonance cavity was attached. Microwave power was adjusted at levels below the saturation condition (2 mW for high-field measurements and 10 mW for low-field measurements). The modulation frequency was 100 kHz, and the modulation amplitude was 0.5 mT; other spectral parameters were adjusted for each spectrum individually. Multiple (150) spectra were acquired to optimize the signal-to-noise ratio, and third-order polynomial averaging was used for subsequent noise reduction. The spectral parameters were obtained with the SIMFONIA software package (Bruker Instruments Inc., Manning Park, Billerica, MA), where coaxial g and hyperfine tensors were assumed. Gaussian line shapes were considered with the line width adjusted for each spectrum. All spectral simulations assumed natural abundance ratios of Cu isotopes. The g values were referenced to diphenylpicryhydrazyl (DPPH, $g = 2.0036$) as an external standard.

TABLE 1: LS Characterization of Empty and SOD-Containing Vesicles

sample	R_g [nm]	R_H [nm]	M [10^8g/mol][a]	A2 [mol/L/g^2][b]
empty vesicles	150 ± 7	156	4.7	5.1×10^{-11}
SOD-containing vesicles	140 ± 10	149	3.4	1.3×10^{-11}

[a] M, weight-average molar mass. [b] A2, second virial coefficient.

SOD Activity Assay. The activity of SOD in the polymeric nanovesicles was investigated by pulse radiolysis with a Febetron 705 (Titan Systems Corp., San Leandro, CA, USA) 2.3 MeV accelerator with a pulse width (fwhm) <50 ns as the radiation source; the optical system consists of a 75 W Xe arc lamp (Hamamatsu, Schüpfen, Switzerland), a 1 or 2 cm optical path quartz cell (Hellma GmbH and Co. KG, Müllheim, Germany), and an Acton SP300i monochromator (Roper Scientific, Ottobrunn, Germany). For signal detection of kinetic traces, a R928 photomultiplier (Hamamatsu) with a DHPCA-200 amplifier (Femto Messtechnik GmbH, Berlin, Germany) with a DL7100 digital storage oscilloscope (Yokogawa Electric Corporation, Tokyo, Japan) is used; a Princeton Instruments PI-MAX 512T gateable ICCD camera (Roper Scientific) is used for detection of time-resolved spectra. $O_2^{\bullet-}$ is formed by irradiation of oxygenated sodium formate (1 M) solutions at pH 8.5. SOD activity is calculated from rates of decay of $O_2^{\bullet-}$, measured at 280 nm, in the presence and absence of SOD. Doses between 10 and 50 Gy/pulse were applied. When experiments with vesicles are carried out, extensive light scattering is observed, which results in a lower signal amplitude. The 100 Hz ripple is caused by the electronic equipment.

Results and Discussion

Formation and Stability of PMOXA−PDMS−PMOXA Vesicles. It has been shown that amphiphilic triblock copolymer PMOXA−PDMS−PMOXA self-assembles spontaneously in dilute aqueous solutions into vesicular structures.[32] Dilute solutions of $PMOXA_{15}-PDMS_{110}-PMOXA_{15}$ form self-assembled nanostructures without encapsulated SOD, which were characterized by TEM, SLS, and DLS experiments. TEM of self-assembled nanostructures of polymer shows circular objects with radii ranging from 50 to 110 nm, in good agreement with results obtained from cryo TEM, which indicated nanovesicles with a radius of 117 nm.[32] TEM measurements repeated after long-term (>3 weeks) storage at 4 °C did not reveal any significant changes, suggesting that the nanovesicles from $PMOXA_{15}-PDMS_{110}-PMOXA_{15}$ are chemically stable.

The LS results are presented in Table 1. We calculate a ratio ($\rho = R_g/R_H$) of the radius of gyration (R_g), obtained from SLS, to the hydrodynamic radius (R_H), from DLS experiments, of 0.96, which is characteristic for hollow spherical objects. On the basis of the assumption of a one-component population, the mean radius of these vesicles is about 150 nm. This larger value is expected, as the R_H from DLS experiments is the sum of the particle and its surrounding hydration sphere.

Formation of PMOXA−PDMS−PMOXA Vesicles with Encapsulated SOD. Nanovesicles prepared with SOD encapsulated were characterized by TEM and LS and compared with empty vesicles. The TEM images for SOD-containing nanoves-

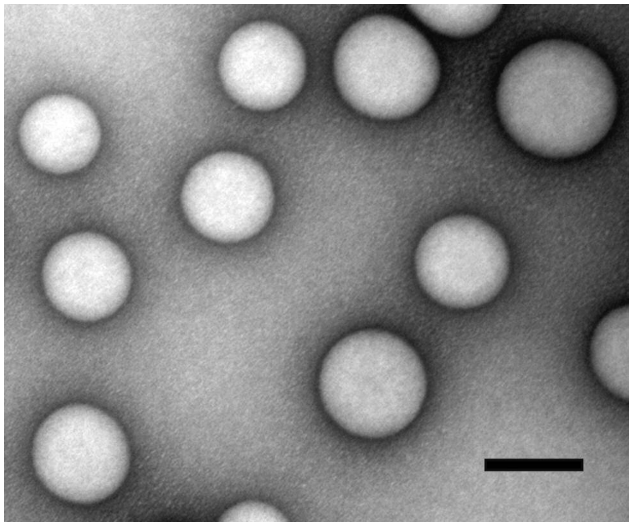

Figure 2. Transmission electron micrograph of SOD-encapsulated in $PMOXA_{15}-PDMS_{110}-PMOXA_{15}$ vesicles (room temperature; scale bar = 200 nm).

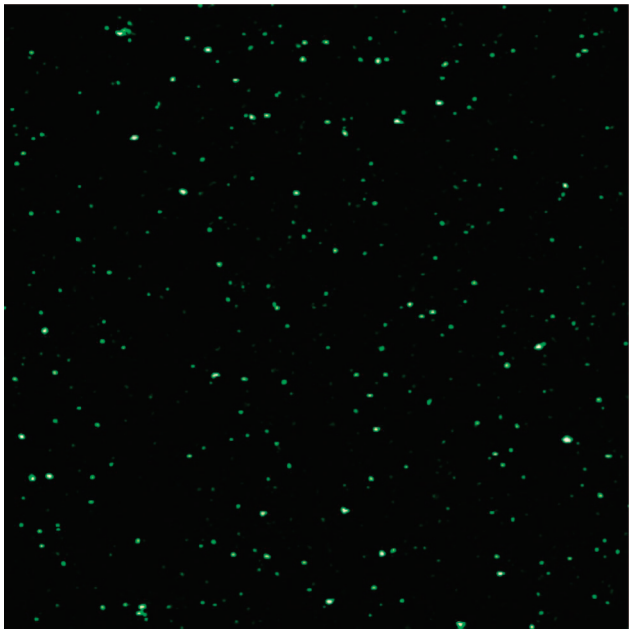

Figure 3. CLSM micrograph of SOD-Alexa Fluor 488 encapsulated in $PMOXA_{15}-PDMS_{110}-PMOXA_{15}$ polymeric nanovesicles.

icles (Figure 2) were essentially identical to those for empty vesicles; additionally, we find a the ratio of $\rho = 0.93$ from SLS and DLS experiments. Taken together, these results indicate that the encapsulation of SOD during the autoassembly process does not influence nanovesicle formation in terms of size or stability.

To investigate whether the protein is located in the inner space of the nanovesicles, a configuration essential for its shielding, we analyzed nanovesicles prepared with encapsulated SOD, labeled with the fluorescence probe Alexa488, by confocal LSM (CLSM) and FCS. CLSM micrographs of encapsulated SOD-Alexa Fluor 488 display a strong fluorescence signal (Figure 3). To verify whether the protein interacts with the surface of the nanovesicles, we examined a purified mixture of empty nanovesicles and free SOD-Alexa Fluor 488 by CLSM. As this purified mixture did not show any fluorescence signal, we conclude that nonspecific interaction between the surface of the empty nanovesicles and the labeled SOD are negligible (data not shown) and that the intense fluorescent signals shown in

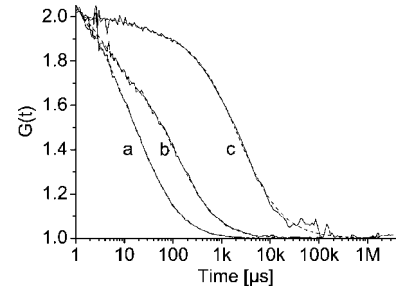

Figure 4. FCS autocorrelation curves. (a) Solution of Alexa Fluor 488 (4×10^{-6} mg/mL) in PBS buffer. (b) Solution of SOD-Alexa Fluor 488 (6×10^{-6} mg/mL) in PBS buffer. (c) Solution of SOD-Alexa Fluor 488 encapsulated in polymeric nanovesicles of $PMOXA_{15}-PDMS_{110}-PMOXA_{15}$. Curves normalized to 2 to facilitate comparison.

the micrograph in Figure 3 are solely from labeled SOD located in the aqueous cavities of the nanovesicles. This is in agreement with previous findings which indicate that the container wall is completely covered by PMOXA chains and shows a very low nonspecific protein binding.[31]

We used FCS to examine in more detail the encapsulation of SOD in nanovesicles, by measuring free Fluor Alexa 488, nonencapsulated SOD-Alexa Fluor 488, and encapsulated SOD-Alexa Fluor 488. In FCS, a special fluctuation correlation approach is applied, in which the laser-induced fluorescence of the excited fluorescent molecules that pass through a very small probe volume is autocorrelated in time to give information about the diffusion times of the molecules. According to the Stokes−Einstein equation, the diffusion times, which are proportional to the R_H of the fluorescent molecules, provide information about interactions of the fluorescent molecules with larger target molecules, including encapsulation of protein in some nanovesicles.[38] The results are presented in Figure 4; autocorrelation amplitudes are normalized to 2 to facilitate comparison of diffusion times and the shapes of the curves. The diffusion time (τ_d) for free Alexa Fluor 488 at room temperature is 23 μs (Figure 4, curve a). For nonencapsulated SOD-Alexa Fluor 488, $\tau_d = 104$ μs, which corresponds to $R_H = 2.4$ nm, in good agreement with the radius of 2.2 nm calculated on the basis of the molecular mass (33 kDa) of SOD-Alexa Fluor 488 (Figure 4, curve b). For encapsulated SOD-Alexa Fluor 488, the multiphasic curve (Figure 4, curve c) indicates the presence of slowly diffusing particles. This population with a reduced diffusion ($\tau_d = 2.3$ ms) represents more than 78% of the total number of fluorescent particles that passes the confocal volume during the measurement time of 30 s and corresponds to vesicles that encapsulate SOD-Alexa Fluor 488. The best fit of the autocorrelation function of the time-dependent fluorescence signal indicates that the remaining diffusing fluorescent particles correspond to free Alexa 488 molecules, which have been encapsulated in vesicles or have not been completely removed from the solution and are detected because of their high quantum yield and the extremely high sensitivity of FCS.[39]

To estimate the number of SOD molecules encapsulated in the nanovesicles, we compared the molecular brightness, reported as count rates per molecule (cpm, in kHz) of free Alexa Fluor 488, nonencapsulated SOD-Alexa Fluor 488, and encapsulated SOD-Alexa Fluor 488. We found that one Alexa Fluor 488 is attached to one SOD molecule by using a calibration curve of molecular fluorescence intensity as function of the known concentrations of Alexa Fluor 488. SOD-Alexa Fluor 488 in the presence of a polymer environment exhibited less

molecular brightness (cpm = 27 kHz) than free Alexa Fluor 488 (cpm = 42 kHz), the difference being mostly attributed to quenching of the dye.[40] In the case of encapsulated SOD-Alexa Fluor 488, the total molecular brightness (cpm_T) corresponds to the weighted sum of the brightnesses of the individual components (cpm_i). By comparing the molecular brightness of the encapsulated SOD-Alexa Fluor 488 solutions with that of the free labeled protein in the presence of polymer, we estimate that an average of 2−5 SOD-Alexa Fluor 488 molecules are encapsulated per nanovesicle when the initial concentration of SOD-Alexa Fluor 488 was 0.1−0.27 mg/mL. This is in agreement with the average number of encapsulated SOD molecules that can be calculated from the initial concentrations of SOD together with the total volume of the inner spaces of the vesicles.The inclusion is a statistical process in which the number of encapsulated molecules is determined by the starting concentrations of the protein. Under the experimental conditions applied, the number of encapsulated SOD molecules is small, as we intended to minimize interactions and functional changes due to confinement in the nanovesicles. In addition, by encapsulating only a small number of SOD molecules, we tested the sensitivity of the nanoreactor, a prerequisite for further therapeutic applications. The study of enzymes at the level of one molecule has the potential to provide significant insight into the detailed spectrum of molecular conformational changes and activities.[41–44]

Structural Stability of PMOXA−PDMS−PMOXA Vesicles Containing SOD-Alexa Fluor 488. The block copolymer membranes can be regarded as mimetics of biological membranes, but they are thicker and far more stable than those of the liposomes.[37,45] To check the stability of the antioxidant nanoreactors, the nanovesicles with encapsulated SOD-Alexa Fluor 488 were reanalyzed by FCS after 3 weeks of storage at 4 °C; no release of encapsulated SOD was observed. Additionally, the LS measurements did not indicate any change in radius or size distribution of the nanoreactors over time (data not shown). This level of stability was expected because of the dimensions of Cu,Zn-SOD and the tightness of the polymer membrane (data not shown). As the vesicles are intended to shield SOD from proteolytic attack, we analyzed the FCS data of a solution of encapsulated SOD-Alexa Fluor 488 to which proteinase K was added in order to see whether the later can attack the encapsulated enzyme. The diffusion time of the vesicles that contain labeled SOD did not change when proteinase K was present, proving that our vesicles protect SOD against enzymatic attack.

Structural and Functional Integrity of the Nanoreactor. In order to investigate whether the encapsulation procedure denatures the protein, we checked for possible geometry changes of the Cu^{II} metal site of the protein by EPR, and characterized the protein's backbone structure by CD. In Cu,Zn-SOD, Cu^{II} is located at the enzyme active site, where it plays a role in the disproportionation of $O_2^{\bullet-}$ to dioxygen and hydrogen peroxide at near diffusion-controlled rates.[46]

It is possible to characterize the first coordination sphere around the metal ion by EPR, from the point of view of both geometry and identification of nuclei with nonzero spin, because the values of spin Hamiltonian parameters can be related to the various distortions of copper environment. Figure 5, curve a shows the frozen-solution EPR spectrum of the encapsulated protein, obtained after a multiple acquisition (more than 500 spectra) procedure. Its simulation derived from a third-order perturbation theory approach (Figure 5, curve b) provides the values of the gyromagnetic and hyperfine tensors: $g_\perp = 2.067$, $g_\parallel = 2.263$, $A_\perp = 4.1$ mT, and $A_\parallel = 13.9$ mT. These values, which are similar to those previously obtained for frozen solutions of bovine Cu,Zn-SOD,[47] indicate that the metal site is not affected by the encapsulation procedure. The metal-binding site of the oxidized form of wild-type Cu,Zn-SOD, as characterized by X-ray diffraction and EPR and electronic spectroscopy, shows the Cu^{II} ion to be five-coordinate, with four histidyl side chains in a tetrahedrally distorted arrangement and one axially situated water molecule.[46,48] Unfortunately, the multiple acquisition procedure required for the encapsulated enzyme impedes the use of either D2-EPR or pulse-EPR methods that would provide more information on the fine details of the coordination sphere of copper.[49]

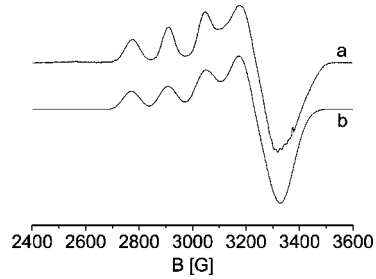

Figure 5. EPR spectra. (a) Cu,Zn-SOD encapsulated in nanovesicles of triblock copolymer $PMOXA_{15}$−$PDMS_{110}$−$PMOXA_{15}$, at 77 K. (b) Simulation derived from a third-order perturbation theory approach.

The CD spectra of SOD-Alexa Fluor 488 before and after being subjected to the encapsulation procedure (Figure S3, Supporting Information) differ only in signal intensity, which is due to sample concentrations. This indicates that if the encapsulation caused any changes to the protein backbone, these changes were reversible.[50]

We performed pulse-radiolysis measurements on series of free and encapsulated SOD samples to determine whether encapsulated SOD remains active. Cu,Zn-SOD is active across a wide functional pH range (5.0−9.5) and under various environmental conditions;[34,51,52] thus, we hypothesized that the protein would not be affected by the encapsulation procedure. Our hypothesis was supported by our observations that encapsulated SOD remains functionally intact. We have previously succeeded in encapsulating other proteins in nanovesicles, for example, β-lactamase and the purine-specific nucleoside hydrolase of *Trypanosoma ViVax* (TvNH), and found that activity was preserved.[53,54] In pulse radiolysis, the kinetics of the dismutation superoxide anions activity is measured directly; the method is sensitive (10 nM), accurate, and reproducible. Figure 6-1 shows the rate of dismutation of the superoxide anion in the presence of empty nanovesicles (curve a, $t_{1/2} \approx 300$ ms) compared to SOD-filled nanovesicles (curve b, $t_{1/2} \approx 4$ ms). The very rapid dismutation of superoxide anions in the presence of encapsulated SOD, together with the finding that SOD is present only in the inner space of the nanovesicles, demonstrates that the nanovesicles are permeable to superoxide and $HO_2^{\bullet}$ and may be described as nanoreactors. The in situ activity assays together with structural characterization of the protein establish that no changes to the protein occur during the encapsulation procedure. The reaction rate of the encapsulated enzyme is similar to that of the free enzyme, which indicates that the diffusion of $O_2^{\bullet-}$ through the triblock copolymer wall is not rate-limiting.

We constructed a calibration curve from a series of pulse-radiolysis determinations of the activity of free SOD in solution (Figure 6-2) and, by assuming free diffusion of superoxide, used the curve to calculate the amount of SOD encapsulated. By taking into account the number of nanovesicles formed in a

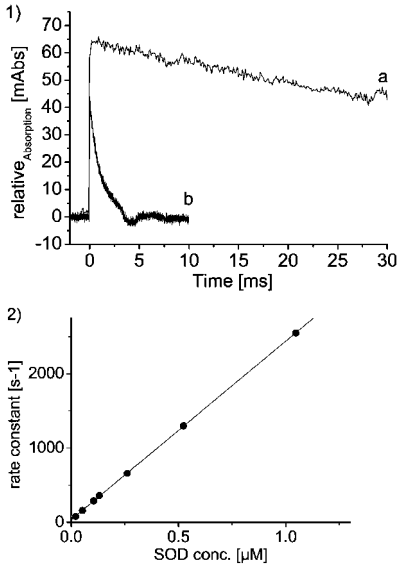

Figure 6. (1) Pulse-radiolysis assay. (a) Uncatalyzed decay observed at 280 nm of 80 μM superoxide produced by a 50 ns pulse of an aerated solution of 1.0 M formate and 10 mM phosphate, pH 8. (b) Superoxide decay catalyzed by SOD (ca. 0.12 μM) encapsulated in $PMOXA_{15}-PDMS_{110}-PMOXA_{15}$ vesicles (10 mg polymer). (2) Pulse-radiolysis standard curve for different concentrations of SOD.

solution of 10 mg/mL of polymer with a weight average molar mass $M = 3.4 \times 10^8$ g/mol (determined from LS experiments) and the concentration of encapsulated SOD (determined by pulse radiolysis), the average encapsulation number is 10 protein molecules/nanovesicle (for an initial concentration of SOD of 0.3 mg/mL). This value is slightly higher than the maximum average number of encapsulated SOD-Alexa Fluor 488 molecules obtained from molecular brightness measurements, where only labeled-SOD molecules are counted (nonlabeled protein molecules are invisible). We emphasize that within the experimental errors and inherent limitations of each method, the results of these two independent methods are in good agreement. Because of the small number of encapsulated SOD molecules, the intermolecular interactions or conformational changes due to confinement of SOD in the nanovesicles can be considered negligible. Because of the mild encapsulation that occurs during the self-assembly process of nanovesicle formation, as well as the experimental conditions aimed at restricting the number of enzyme molecules encapsulated, SOD remains fully active and the dismutation of superoxide takes place in the inner space of the nanoreactor.

According to studies of the permeability of bilayer lipid membranes to superoxide radicals, the transport of $O_2^{\bullet -}$ is strongly dependent on the structural state of the membrane and on the localization of the substrate; the permeability coefficient is estimated at $2.1 \times 10^{-6}-7.6 \times 10^{-8}$ cm/s in lipids.[55,56] Generally, for lipid bilayers, channels for anion transport must be incorporated, and the bilayers tend to break down and release encapsulated compounds over time. However, the polymeric nanoreactors described here are permeable to both dioxygen and superoxid and do not require anion channels.[16,17,54,57] Because the protein is acting inside the polymer vesicles, our nanoreactor is inherently simpler and avoids the problems connected to an efficient release in the body that are specific for conventional carriers, such as liposomes and other polymeric nanocontainers. The antioxidant nanoreactor is not limited to use with SOD; it can be chemically modified for specific targeting approaches and permits the simultaneous encapsulation of other proteins to extend its applicability.

Conclusion

We have designed and tested a novel antioxidant nanoreactor based on encapsulation of SOD in superoxide-permeable nanovesicles. The SOD encapsulated in block copolymer nanovesicles formed via self-assembly is located in the inner cavity of the nanovesicles, and the mild encapsulation process does not affect the structural or functional integrity of the enzyme. The polymeric membrane of the nanovesicles is capable of both protecting the encapsulated SOD and allowing penetration of the inner space by $O_2^{\bullet -}$, where the conversion to hydrogen peroxide and oxygen is catalyzed. Compared with conventional drug nanocarriers made of liposomes or polymers, our system combines the advantages of a polymer shield with an in situ active protein. The tight polymeric membrane of the nanovesicles prevents release of the encapsulated protein from the nanoreactor.[32] The sensitivity of this nanoreactor is high, as proved by the observation that SOD activity was measured although the number of encapsulated SOD molecules is small. The production of the nanoreactor is straightforward, involving simple self-assembly of the amphiphilic copolymer in the presence of the protein. The level of superoxide permeability obviates the necessity of inserting artificial channels in the polymer membrane, as usually done in nanoreactors.[16,17,54,57] The antioxidant nanoreactors remain stable over several weeks of storage at 4 °C. The selective permeability of the polymeric membrane may be generally useful to improve the bioavailability of proteinasceous pharmaceuticals.

Acknowledgment. This work was supported by the *Swiss National Science Foundation* (Project no. 200021-115956/1) and by Polyamphi, NCCR Nanosciences (MRTN-CT-2003-505027), and this is gratefully acknowledged. The authors thank Dr. P.L. Bounds from ETH Zurich for very useful discussions and for reading the manuscript. C.G.P. and F.A. thank M. Grzelakowski from Basel University for providing the polymer. C.G.P. wishes to thank EPR group at ETH Zurich for providing EPR facilities and Dr. S. K. Hillman for reading the manuscript.

Supporting Information Available: Figure S1 shows a transmission electron micrograph of empty $PMOXA_{15}-PDMS_{110}-PMOXA_{15}$ vesicles. Figure S2 shows a Zimm plot of polymer vesicles without encapsulated SOD. Figure S3 shows CD spectra of SOD-Alexa Fluor 488 separated from SOD-filled nanovesicles by SEC and SOD-Alexa Fluor 488 not exposed to the encapsulation conditions. This material is available free of charge via the Internet at http://pubs.acs.org.

References and Notes

(1) Beckman, J. S.; Koppenol, W. H. *Am. J. Physiol.* **1996**, *271*, C1424–37.

(2) Cabelli, D. E.; Riley, D.; Rodriguez, J. A.; Valentine, J. S.; Zhu, H. In *Biomimetic Oxidations Catalyzed by Transition Metal Complexes*; Meunier, B., Ed.; Imperial College Press/World Scientific: London, 2000; pp 461−508.

(3) Droege, W. *Oxidative Stress, Disease and Cancer;* **2006**, 885–895.

(4) Regnault, C.; Soursac, M.; Roch-Arveiller, M.; Postaire, E.; Hazebroucq, G. *Biopharm. Drug Dispos.* **1996**, *17*, 165–74.

(5) Jadot, G.; Vaille, A.; Maldonado, J.; Vanelle, P. *Clin. Pharmacokinet.* **1995**, *28*, 17–25.

(6) Kang, J. H.; Kim, K. S.; Choi, S. Y.; Kwon, H. Y.; Won, M. H.; Kang, T.-C. K. *Biochim. Biophys. Acta* **2002**, *1570*, 89–96.

(7) Maksimenko, A. V. *Curr. Pharm. Des.* **2005**, *11*, 2007–16.

(8) Maksimenko, A. V.; Tischenko, E. G. K. *Biochemistry* **1997**, *62*, 1163–1166.

(9) Corvo, M. L.; Boerman, O. C.; Oyen, W. J. G.; Jorge, J. C. S.; Cruz, M. E. M.; Crommelin, D. J. A.; Storm, G. K. *Pharm. Res.* **2000**, *17*, 600–606.

(10) Estevez, A. G.; Sampson, J. B.; Zhuang, Y. X.; Spear, N.; Richardson, G. J.; Crow, J. P.; Tarpey, M. M.; Barbeito, L.; Beckman, J. S. *Free Radical Biol. Med.* **2000**, *28*, 437–446.
(11) Rengel, R. G.; Filipovic-Grcic, J.; Cepelak, I.; Zanic-Grubisic, T.; Barisic, K. K. *Eur. J. Pharm. Biopharm.* **2005**, *60*, 47–51.
(12) Saifer, M. G. P.; Somack, R.; Williams, L. D. *Adv. Exp. Med. Biol.* **1994**, *366*, 377–87.
(13) Barenholz, Y. *Curr. Opin. Colloid Interface Sci.* **2001**, *6*, 66–77.
(14) Fonseca, M. J.; Alsina, M. A.; Reig, F. *Biochim. Biophys. Acta* **1996**, *1279*, 259–65.
(15) Fidler, I. J.; Raz, A.; Fogler, W. E.; Kirsh, R.; Bugelski, P.; Poste, G. *Cancer Res.* **1980**, *40*, 4460–6.
(16) Vriezema, D. M.; Aragones, M. C.; Elemans, J. A. A. W.; Cornelissen, J. J. L. M.; Rowan, A. E.; Nolte, R. J. M. *Chem. Rev.* **2005**, *105*, 1445–1489.
(17) Vriezema, D. M.; Hoogboom, J.; Velonia, K.; Takazawa, K.; Christianen, P. C. M.; Maan, J. C.; Rowan, A. E.; Nolte, R. J. M. *Angew. Chem., Int. Ed.* **2003**, *42*, 772–776.
(18) Choi, H.-J.; Montemagno, C. D. *Nano Lett.* **2005**, *5*, 2538–2542.
(19) Kishimura, A.; Koide, A.; Osada, K.; Yamasaki, Y.; Kataoka, K. *Angew. Chem., Int. Ed.* **2007**, *46*, 6085–6088.
(20) Vriezema, D. M.; Garcia, P. M. L.; Oltra, N. S.; Natzakis, N. S.; Kuiper, S. M.; Nolte, R. J. M.; Rowan, A. E.; van Hest, J. C. M. *Angew. Chem., Int. Ed.* **2007**, *46*, 7378–7382.
(21) Discher, D. E.; Eisenberg, A. *Science* **2002**, *297*, 967–973.
(22) Herrero-Vanrell, R.; Rincon, A. C.; Alonso, M.; Reboto, V.; Molina-Martinez, I. T.; Rodriguez-Cabello, J. C. *J. Controlled Release* **2005**, *102*, 113–122.
(23) Kita-Tokarczyk, K.; Grumelard, J.; Haefele, T.; Meier, W. *Polymer* **2005**, *46*, 3540–3563.
(24) Antonietti, M.; Foerster, S. *Adv. Mater.* **2003**, *15*, 1323–1333.
(25) Discher, B. M.; Won, Y.-Y.; Ege, D. S.; Lee, J. C. M.; Bates, F. S.; Discher, D. E.; Hammer, D. A. *Science* **1999**, *284*, 1143–1146.
(26) Palivan, C. G.; Vebert, C.; Axthelm, F.; Meier, W. *Nanotechnol. Biol. Med.* **2007**, 32/1–32/26.
(27) Giovagnoli, S.; Luca, G.; Casaburi, I.; Blasi, P.; Macchiarulo, G.; Ricci, M.; Calvitti, M.; Basta, G.; Calafiore, R.; Rossi, C. *J. Controlled Release* **2005**, *107*, 65–77.
(28) Lee, S.; Yang, S. C.; Heffernan, M. J.; Taylor, W. R.; Murthy, N. *Bioconjug. Chem.* **2007**, *18*, 4–7.
(29) Hirt, T.; Baron, R. C.; Lohmann, D.; Meier, W. P. Novartis, Zwitzerland;Application: US patent, 2000.
(30) Broz, P.; Benito Samantha, M.; Saw, C.; Burger, P.; Heider, H.; Pfisterer, M.; Marsch, S.; Meier, W.; Hunziker, P. *J. Controlled Release* **2005**, *102*, 475–88.
(31) Woodle, M. C.; Engbers, C. M.; Zalipsky, S. *Bioconjug. Chem.* **1994**, *5*, 493–6.
(32) Kumar, M.; Grzelakowski, M.; Zilles, J.; Clark, M. M.; Meier, W. *Proc. Natl. Acad. Sci. U. S. A.* **2007**, *104*, 20723–8.
(33) Nardin, C.; Hirt, T.; Leukel, J.; Meier, W. *Langmuir* **2000**, *16*, 1035–1041.
(34) Michel, E.; Nauser, T.; Sutter, B.; Bounds, P. L.; Koppenol, W. H. *Arch. Biochem. Biophys.* **2005**, *444*, 76.
(35) Williams, G.; Watts, D. C.; Dev, S. B.; North, A. M. *Trans. Faraday Soc.* **1971**, *67*, 1323–35.
(36) Van Zanten, J. H. *Surfactant Sci. Ser.* **1996**, *62*, 239–294.
(37) Nardin, C.; Winterhalter, M.; Meier, W. *Langmuir* **2000**, *16*, 7708–7712.
(38) Rigler, P.; Meier, W. K. *J. Am. Chem. Soc.* **2006**, *128*, 367–373.
(39) Schwille, P.; Korlach, J.; Webb, W. W. *Cytometry* **1999**, *36*, 176–182.
(40) Rajagopalan, P. T. R.; Zhang, Z.; McCourt, L.; Dwyer, M.; Benkovic, S. J.; Hammes, G. G. *Proc. Natl. Acad. Sci. U. S. A.* **2002**, *99*, 13481–13486.
(41) Comellas-Aragones, M.; Engelkamp, H.; Claessen, V. I.; Sommerdijk, N. A. J. M.; Rowan, A. E.; Christianen, P. C. M.; Maan, J. C.; Verduin, B. J. M.; Cornelissen, J. J. L. M.; Nolte, R. J. M. *Nat. Nanotechnol.* **2007**, *2*, 635–639.
(42) Flomenbom, O.; Velonia, K.; Loos, D.; Masuo, S.; Cotlet, M.; Engelborghs, Y.; Hofkens, J.; Rowan, A. E.; Nolte, R. J. M.; Van der Auweraer, M.; De Schryver, F. C.; Klafter, J. *Proc. Natl. Acad. Sci. U. S. A.* **2005**, *102*, 2368–2372.
(43) Roeffaers, M. B. J.; De Cremer, G.; Uji-i, H.; Muls, B.; Sels, B. F.; Jacobs, P. A.; De Schryver, F. C.; De Vos, D. E.; Hofkens, J. *Proc. Natl. Acad. Sci. U. S. A.* **2007**, *104*, 12603–12609.
(44) Boukobza, E.; Sonnenfeld, A.; Haran, G. *J. Phys. Chem. B* **2001**, *105*, 12165–12170.
(45) Bermudez, H.; Brannan, A. K.; Hammer, D. A.; Bates, F. S.; Discher, D. E. *Macromolecules* **2002**, *35*, 8203–8208.
(46) Hough, M. A.; Hasnain, S. S. *J. Mol. Biol.* **1999**, *287*, 579–592.
(47) Palivan, C. G.; Palivan, H.; Goodman, B. A. *Proc. R. Soc. Edinburgh, Sect. B* **1994**, *102*, 273–7.
(48) Palivan, C. G.; Goodman, B. A. *Recent Res. Dev. Inorg. Organomet. Chem.* **2001**, *1*, 141–159.
(49) Schweiger, A.; Jeschke, G. *Principles of Pulse Electron Paramagnetic Resonance Spectroscopy*; Oxford University Press: New York, 2001.
(50) Greenfield, N. J. *Trends Anal. Chem.* **1999**, *18*, 236–244.
(51) Ellerby, L. M.; Cabelli, D. E.; Graden, J. A.; Valentine, J. S. *J. Am. Chem. Soc.* **1996**, *118*, 6556–6561.
(52) Fridovich, I. *J. Biol. Chem.* **1997**, *272*, 18515–7.
(53) Ranquin, A.; Versees, W.; Meier, W.; Steyaert, J.; Van Gelder, P. *Nano Lett.* **2005**, *5*, 2220–2224.
(54) Nardin, C.; Thoeni, S.; Widmer, J.; Winterhalter, M.; Meier, W. *Chem. Commun.* **2000**, 1433–1434.
(55) Gus'kova, R. A.; Ivanov, I. I.; Kol'tover, V. K.; Akhobadze, V. V.; Rubin, A. B. *Biochim. Biophys. Acta* **1984**, *778*, 579–85.
(56) Takahashi, M.; Asada, K. *Arch. Biochem. Biophys.* **1983**, *226*, 558–66.
(57) Broz, P.; Driamov, S.; Ziegler, J.; Ben-Haim, N.; Marsch, S.; Meier, W.; Hunziker, P. *Nano Lett.* **2006**, *6*, 2349–2353.

JP803032W